

Research Paper

Cite this article: Abed AT, Singh MSJ, Jawad AM (2020). Investigation of circular polarization technique in Q-slot antenna. *International Journal of Microwave and Wireless Technologies* **12**, 176–182. <https://doi.org/10.1017/S1759078719001107>

Received: 24 November 2018

Revised: 22 July 2019

Accepted: 23 July 2019

First published online: 20 August 2019


Key words:

Circularly polarized and axial ratio bandwidth; Q-slot antenna

Author for correspondence:

Amer T. Abed, E-mail: amer.t.abed@ieee.org

Investigation of circular polarization technique in Q-slot antenna

Amer T. Abed¹ , Mandeep S. J. Singh² and Aqeel M. Jawad³

¹Department of communication Engineering, Al-M'mamon University College, Baghdad, Iraq; ²Faculty of Engineering and Built Environment Universiti Kebangsaan Malaysia (UKM), Selangor, Malaysia and ³Department of Computer Communication Engineering, Al-Rafidain University College, Baghdad, Iraq

Abstract

This paper describes and analyzes a new technique used in Q-slot antenna to generate circular polarization (CP). The CP characteristics were investigated carefully by studying the surface current distribution, the phase difference between the left hand circular polarization (LHCP) and right hand circular polarization (RHCP) at some resonant frequencies, and the measured values of the axial ratio bandwidth (ARBW). Normal arms (E_1 and E_2) were cut in the upper elliptical feeding strip line to form an open-mouth structure. The arms E_1 and E_2 were made equal in length and set perpendicular to each other to have normal electric fields, leading to the generation of CP radiation. A formula was modified for the dual resonant frequencies f_1 , f_2 of the modes TM_{010} and TM_{001} . The measured values of the ARBW indicated that the antenna has a wide ARBW of 4.8–5.93 GHz, which is approximately 52% of the 3rd operating band of 4.7–6.8 GHz. The wide ARBW in a small size indicated that the design of the Q-slot antenna overcame the limits of designing antennas with wide ARBW in small size and low profile. A formula for normalized field was driven according to the complementarity of the Q-slot antenna.

Introduction

Transmitting and receiving signals with the same polarization in portable communication devices that apply linear polarization for size reduction is difficult. The problem worsens when the antenna is used to operate at multiple bands. Circular polarization (CP) antennas are currently used in modern communication systems to avoid many serious problems, such as mismatch polarization and multipath interferences [1]. Researchers have used many techniques to generate CP radiation; these methods include using two orthogonal modes with a 90° time–phase difference between them to excite the antenna [1]; rotating the radiator [2] or the slot [3] with respect to the diagonal of the patch to create a required phase shift to generate CP radiation; using the termination circuit of a capacitor or inductor serial/parallel tank to produce CP of two types (LHCP and RHCP) [4]; and using special structures in designing antennas to generate CP radiation characteristics, such as the Amer fractal slot [5] and the Fibonacci spiral structure [6].

This study aims to investigate the CP characteristics of the Q-slot antenna by three methods, studying the distribution of surface current, the phase difference between left and right polarization at some resonant frequencies and the measured values of the axial ratio bandwidth (ARBW).

CP technique

This study investigates the CP technique used in the slot antenna reported in [7]. The method is presented in Fig. 1 [7]. The proposed slot antenna uses the ground-slotted technique, where a Q-shaped slot is cut in the ground plate, which comprises a strip line that is provided different width and length dimensions to excite the antenna through a step impedance strip line to generate many resonant frequencies. These frequencies are collected together to have multi-operating bands that cover Wireless Fidelity (Wi-Fi) and Worldwide Interoperability for Microwave Access (WiMAX) requirements.

A new technique is used to generate CP radiation by cutting normal arms (E_1 and E_2) in an elliptical upper strip feeding line F_3 to generate the modes (TM_{010} and TM_{001}), the mode TM_{001} produces far-field in Y-direction E_y while the other mode produces far-field in X-direction E_x , which are needed to have CP characteristics. With a simulation of surface current distribution, the function of each part of the proposed antenna structure can be examined. Both electric fields (E_y and E_x) are linearly polarized in Y and X directions [8].

$$E_y = c \frac{\sin((\pi/E_1)y')}{k^2(1 - j/Q_t) - (k_y)^2}, \quad (1)$$

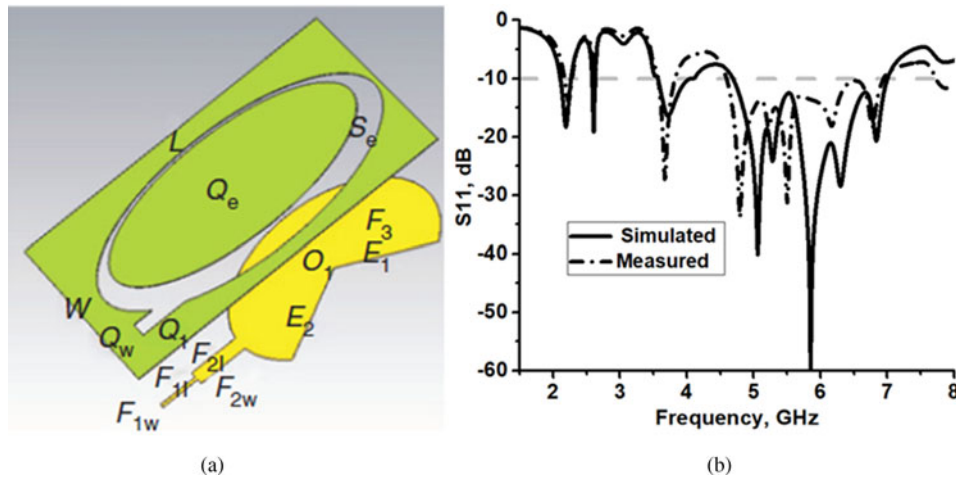


Fig. 1. The Q-slot antenna. (a) Geometry of the Q-Slot antenna. (b) The impedance bandwidth of the Q-Slot antenna [7].

$$E_x = c \frac{\sin((\pi/E_2)z')}{k^2(1 - j/Q_t) - (k_z)^2}, \tag{2}$$

$$k_y = \frac{\pi}{E_1}, k_x = \frac{\pi}{E_2} \tag{3}$$

where $Q_t = 1/\tan\delta$ is the quality factor, and c is the speed of the light in free space. k_y and k_x are the propagation constants in Y and X directions. If the feed point is selected to be at (y', X') along the major axis of the elliptical strip feeding line F_3 , the arms E_1 and E_2 can be represented as

$$\frac{y'}{E_1} = \frac{X'}{E_2}. \tag{4}$$

At the broad side of the electric fields E_y and E_x can be formed

$$\frac{E_y}{E_x} \approx \frac{k(1 - j/2Q_t) - (k_y)}{k(1 - j/2Q_t) - (k_x)}, \tag{5}$$

when the numerator and denominator in equation (5) are equals and out of phase 90° , the CP can be achieved and that can happen when

$$E_y - E_x = k_x - k_y = 0, \tag{6}$$

k_x and k_y are equal in amplitude and out of phase by 90° . The dual resonant frequencies f_1, f_2 of the modes TM_{010} and TM_{001} selected by the arms E_1 and E_2 .

$$f_1 = \frac{f_0}{\sqrt{1 + 1/Q_t}}, \tag{7}$$

$$f_2 = f_0 \sqrt{1 + \frac{1}{Q_t}}, \tag{8}$$

where f_0 is the center frequency of the bandwidth $(f_2 - f_1)$, $\tan\delta$ equals to 4.3 for substrate FR-4. According to equations (7) and (8), $f_1 = 4.8$ GHz while $f_2 = 6.1$ GHz.

Investigation of CP

The CP characteristics of the Q-slot antenna will be investigated carefully by three methods; studying the distribution of surface current, the phase difference between left and right polarization at some resonant frequencies and the measured values of the ARBW.

Surface current distribution

The current distribution of the resonant frequencies is simulated by the software (CST), as shown in Fig. 2. The maximum current is concentrated at the narrow edge of the slot in the ground plane for all resonant frequencies due to the main intensity of the surface current at the left edge of the oval strip F_3 , which is near the narrow edge of the slot, while the current distribution on the radiation plate ($F_1, F_2,$ and F_3) depends on the resonant frequency. At a low resonant frequency 2.5 GHz (Fig. 2(a)), the current is mainly concentrated along the strips F_1 and f_2 ; the summation of the lengths f_{1l} and f_{2l} is equal to 22 mm, which is approximately a quarter of the wavelength for the resonant frequency of 2.5 GHz. At 3.5 GHz, most of the current is on the feed strips F_1, f_2 , and the lower part of F_3 . This condition means that the 1st and 2nd operating bands are affected significantly by the dimensions of the lower and middle feed lines f_1 and f_2 . At the upper operating band 4.7–6.8 GHz (Figs 2(b) and 2(c)), the intensity of the surface current along the feeding line increases, especially at the resonant frequency 5.8 GHz, compared with that at the low operating bands because the summation of lengths f_{1l}, f_{2l} , and the circumference of F_3 is equal to 61 mm, which matches the wavelength of the frequency 5.8 GHz. The current is concentrated on the ground plane at the narrow edge of the slot S_e and near the slot Q_w , as shown in Figs 2(b) and 2(c) (at resonant frequencies 5 and 5.8 GHz, respectively). This finding means that the upper band is affected by the dimensions of the slot Q_w and the width of the slot S_e , which is directly affected by the location of the elliptical shape Q_e .

Three nulls are observed in the current distribution at the resonant frequency 5 GHz (Fig. 2(b)). Meanwhile, four nulls are

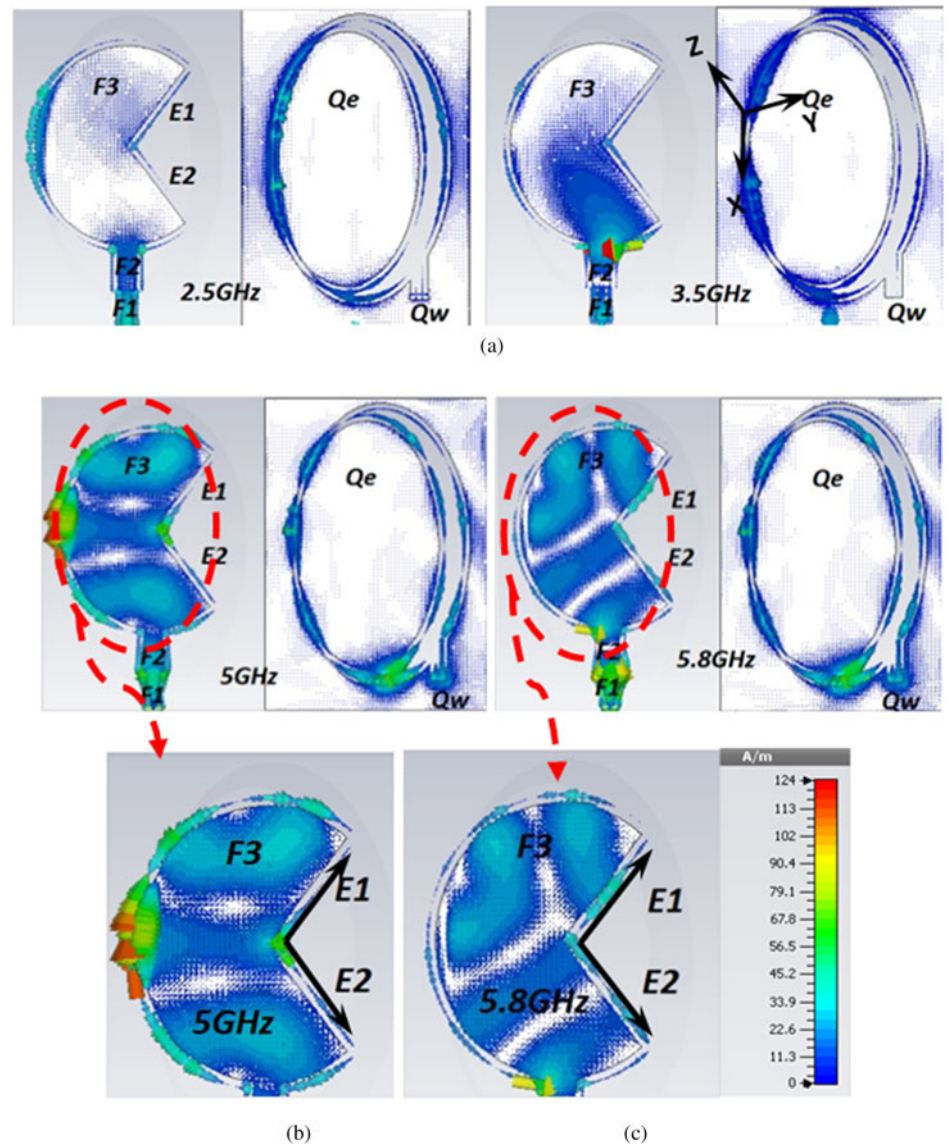


Fig. 2. Surface current distribution. (a) At 2.5 and 3.5 GHz. (b) At 5 GHz. (c) At 5.8 GHz.

observed at 5.8 GHz. Figures 2(b) and 2(c) present the surface current distributions at 5 and 5.8 GHz along F_3 , which explain the aim of using perpendicular arms E_1 and E_2 in an elliptical shape F_3 . The surface current along the arms E_1 and E_2 have two components that seem normal to each other, especially at resonant frequencies 5 and 5.8 GHz. These normal components generate normal components of the field, which are necessary in radiating CP. At lower resonant frequencies of 2.5 and 3.5 GHz (Fig. 2(a)), the surface current either does not exist along the arms E_1 and E_2 or exists with low intensity, which means that the proposed antenna has CP at the upper band only.

Left- and right-hand polarization

The left- and right-hand polarization patterns on the E -Plane (when $\theta = 90^\circ$) are illustrated in Fig. 3 at the resonant frequencies of 2.5, 3.5, 5, and 5.8 GHz. The phase difference between the left- and right-hand polarization patterns is 170° at 2.5 GHz (Fig. 3(a)) and reduces to 70° at 3.5 GHz (Fig. 3(b)). Thus, no CP

radiation exists at resonant frequencies 2.5 and 3.5 GHz, this study matched with the surface current distribution shown in Fig. 2(a).

The left and right polarization at 5 and 5.8 GHz are almost perpendicular to each other as shown in Figs 3(c) and 3(d), this result agrees with the current distribution along the arms E_1 and E_2 as it is shown in Figs 2(b) and 2(c) where two normal components of the surface current observed produce CP at the upper operating band. In another meaning, the values of ARBW are <3 dB during the upper band only. The left- and right-hand radiation at all resonant frequencies had asymmetrical shapes because the Q-slot in ground plane is asymmetrical, which causes different paths of the surface current when changing the phase of excited signal.

Axial ratio bandwidth

Figure 4 presents the measured values of the ARBW for different types of cutting in the upper feed line F_3 . The AR values for circular cutting (red curve) and without cutting (blue curve) are

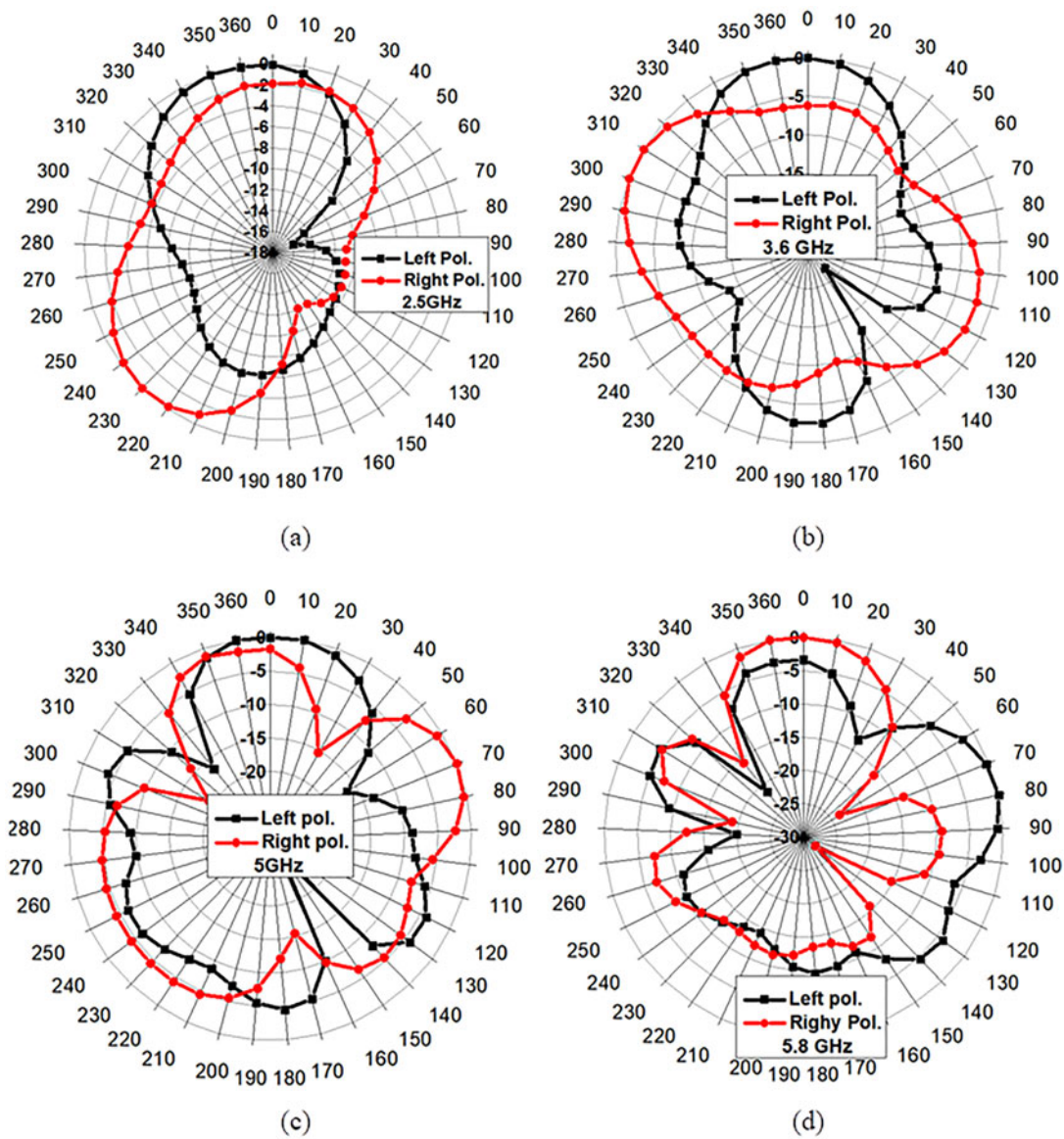


Fig. 3. Left (black curves) and right-hand (red curves) polarization patterns in *E*-Plane. (a) At 2.5 GHz. (b) At 3.5 GHz. (c) At 5 GHz. (d) At 5.8 GHz.

considerably greater than the AR value required for CP generation (<3 dB). Nearly no current distribution is present along the perpendicular arms E_1 and E_2 at 2.5 and 3.5 GHz. In using an open-end mouth slot with perpendicular arms E_1 and E_2 in F_3 , the AR values decrease for the frequency spectrum 2–7 GHz, especially at the 3rd operating band. ARBW is <3 dB at 4.8–5.93 GHz (black curve in Fig. 4), which is approximately 52% of the 3rd band of 4.7–6.8 GHz. The ARBW values shown in Fig. 4 match the above studies about the surface current distribution in Fig. 2 and the LHP–RHP represented in Fig. 3.

Radiation fields

The Q-slot is almost similar to the elliptical slot. Therefore, its radiation pattern will be likened to the radiating antenna for the elliptical slot. According to the previous study, the complementary antenna for the elliptical slot is the elliptical loop. As it is shown in Fig. 5. In rectangular coordinates, the ellipse can be

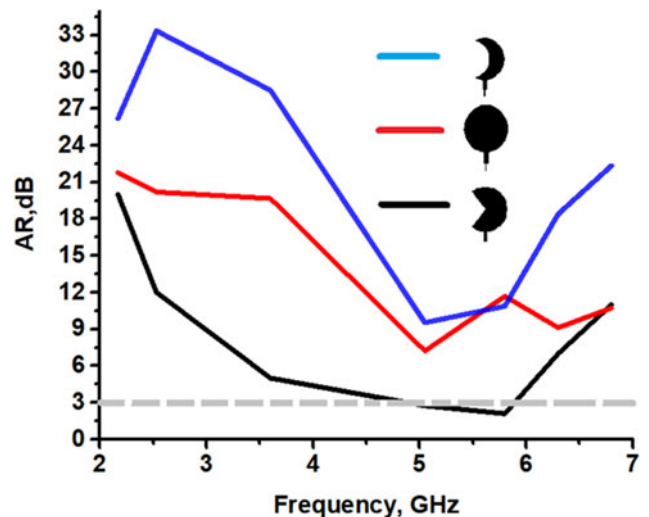


Fig. 4. Measured AR for different types of cuts in strip line F_3 .

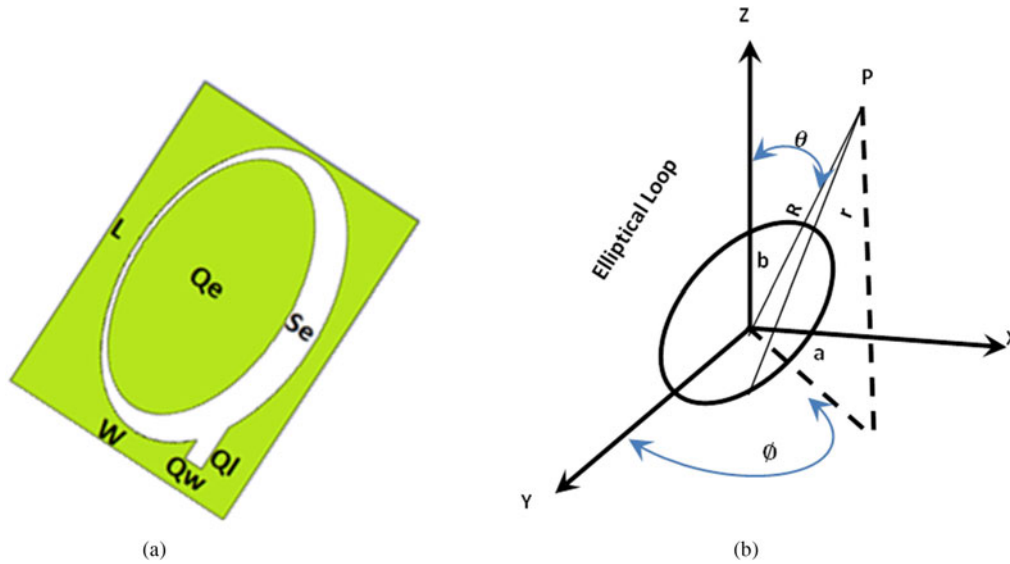


Fig. 5. The Q-slot and the complementary. (a) Q-slot. (b) The complementary.

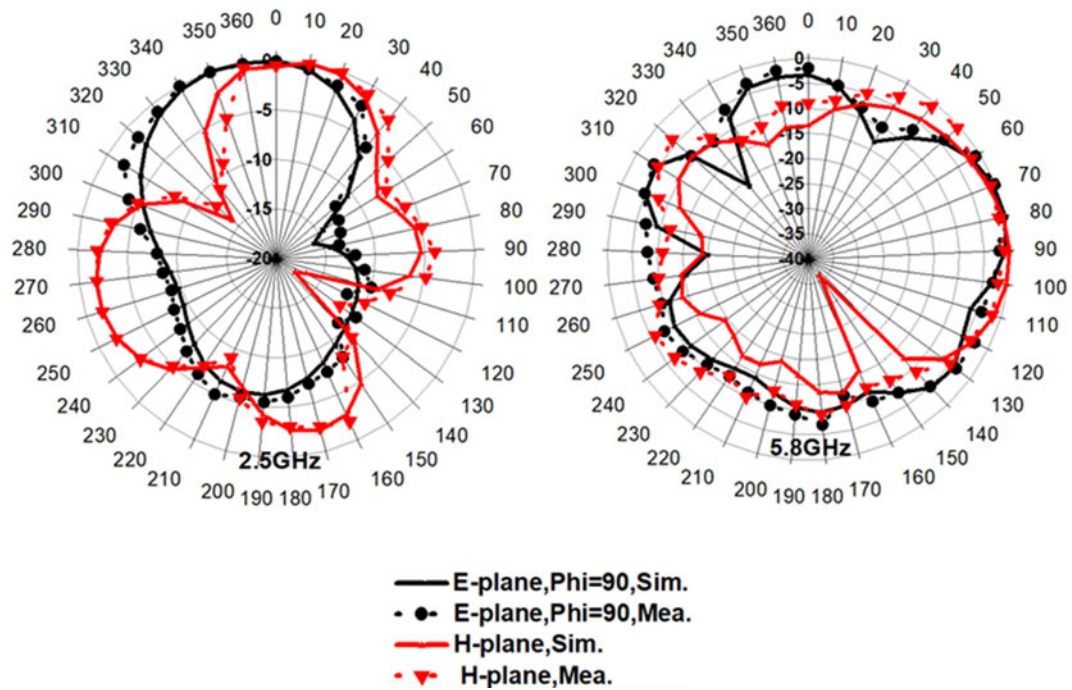


Fig. 6. The simulated and measured radiation fields in E and H-plane.

presented by the following parameters

$$X = a \cos u, Y = b \sin u, -\pi \leq u \leq \pi, \quad (9)$$

where a, b are the minor and major axes of the ellipse. In terms of rectangular coordinates, the x component of the Hertzian vector potential at point P can be written as [8]

$$A_x = \frac{e^{-i\beta R}}{i4\pi R w \epsilon} \int_{u=-\pi}^{u=\pi} I_o e^{[ik(x \cos \theta \sin \theta + y \sin \theta \sin \theta)]} dx, \quad (10)$$

where I_o is the current in ds (an element length) = $2\pi/\lambda$.

By substituting equation (9) in equation (10)

$$A_x = \frac{-I_o a e^{-i\beta R}}{i4\pi R w \epsilon} \int_{-\pi}^{\pi} e^{[ik(a \cos u \cos \theta \sin \theta + b \sin u \sin \theta \sin \theta)]} \sin u du. \quad (11)$$

Let

$$\begin{aligned} \gamma &= \tan^{-1}\left(\frac{b}{a} \tan \theta\right) \text{ and } \delta \\ &= ka \sin \theta \sqrt{(\cos^2 \theta + (b/a)^2 \sin^2 \theta)}. \end{aligned} \quad (12)$$

Equation (10) reduced to

$$A_x = \frac{-I_o a e^{-i\beta R}}{i4\pi R w \epsilon} \int_{-\pi}^{\pi} e^{[i\delta(\cos u - \gamma)]} \sin u du. \quad (13)$$

The term $e^{[i\delta(\cos u - \gamma)]}$ can be expanded by Fourier series with Bessel function and equation (13) simplified to

$$A_x = \frac{-I_o a e^{-i\beta R}}{2R w \epsilon} J_1(\delta) \sin(\gamma). \quad (14)$$

By the same method the Y component can be driven

$$A_y = \frac{-I_o a e^{-i\beta R}}{2R w \epsilon} J_1(\delta) \cos(\gamma). \quad (15)$$

In spherical coordinates

$$A_\theta = A_x \cos \theta \cos \vartheta + A_y \cos \theta \sin \vartheta, \quad (16)$$

$$A_\vartheta = -A_x \sin \vartheta + A_y \cos \vartheta. \quad (17)$$

After substituting the spherical components become

$$A_\theta = 0. \quad (18)$$

The electric field component can be driven by applying the following vector relationship

$$A_\vartheta = \frac{I_o a e^{-i\beta R}}{2R w \epsilon} J_1(\delta) \sqrt{(\sin^2 \gamma + (b/a)^2 \cos^2 \gamma)}. \quad (19)$$

That means there is no θ component for the Hertzian vector, or the current in the elliptical loop has only ϑ component i.e. the radiation is outside the loop.

$$E_\vartheta = w^2 \mu \epsilon A_\vartheta + \nabla(\nabla \cdot A_\vartheta), \quad (20)$$

$$E_\vartheta = \frac{I_o k a e^{-i\beta R}}{2R} J_1(\delta) \sqrt{(\sin^2 \gamma + (b/a)^2 \cos^2 \gamma)}. \quad (21)$$

The first-order Bessel function can be equal to

$$J_1(x) = \frac{1}{2} x. \quad (22)$$

The normalized field for elliptical loop

$$F_\vartheta = \delta \sqrt{(\sin^2 \gamma + (b/a)^2 \cos^2 \gamma)}. \quad (23)$$

From equation (23), the radiation pattern for elliptical loop which is complementary of the elliptical slot depends on the size (values of a and b) and the pattern is non-uniform, for the small elliptical slot ($a \approx b$), the normalized field will be

$$F_\vartheta = kb \sin(\theta). \quad (24)$$

Therefore, the radiation pattern for a small elliptical slot depends on ϑ and seems to be circular. But the desired Q-slot antenna is asymmetrical, so the radiation pattern will be asymmetrical also. However, for the small slot, it was demonstrated that the radiation pattern is independent of the shape, and it is almost circular. Consequently, the radiation pattern of the small elliptical slot in the H-plane is independent of the angle (ϑ) and therefore, it is omnidirectional. But all radiation patterns in H-plane represented in Fig. 6 are not omnidirectional due to the asymmetrical slots used in the proposed antenna, that is a narrow slot on the left side and a wide slot on the right side as shown in Fig. 1, which caused asymmetrical current distribution.

Conclusion

Clearly, the CP technique used in the Q-slot antenna is new, where in normal arms (E_1 and E_2) in an elliptical upper strip feeding line have been cut to generate CP characteristics with wide ARBW in small size and low profile. Therefore, this technique overcame the limits of generating CP with wide ARBW. Notably, the driven formula for normalized field shows that the radiation pattern for the small slot is independent of the slot shape.

Acknowledgement. The authors would like to thank Al-Rafidain University College, Baghdad, Iraq for supporting this research.

References

1. **Abed AT, Singh MJ and Islam MT** (2017) Dual crescent-shaped slot antenna fed by circular polarization into dual orthogonal strip line. *IET Microwaves, Antennas & Propagation* **11**, 2129–2133.
2. **Ge L, Sim CD, Su HL, Lu JU and Ku C** (2018) Single-layer dual-broadband circularly polarized annular-slot antenna for Wlan applications. *IET Microwaves, Antennas & Propagation* **12**, 99–107.
3. **Wangwang H, Yang F, Long R, Zhou L and Yan F** (2016) Single-fed low-profile high-gain circularly polarized slotted cavity antenna using a high-order mode. *IEEE Antennas and Wireless Propagation Letters* **15**, 110–113.
4. **Zhou CF and Cheung SW** (2017) A wideband CP crossed slot antenna using $1-\lambda$ resonant mode with single feeding. *IEEE Transactions on Antennas and Propagation* **65**, 4268–4273.
5. **Abed AT, Singh MJ and Islam MT** (2016) Amer Fractal Slot Antenna with Quad Operating Bands High Efficiency for Wireless Communication. The IEEE 3rd International Symposium on Telecommunication Technologies (ISTT), Malaysia, pp. 6–8.
6. **Chetna Sharma SM and Vishwakarma DK** (2017) Miniaturization of spiral antenna based on fibonacci sequence using modified Koch curve. *IEEE Antennas and Wireless Propagation Letters* **16**, 932–935.
7. **Abed AT and Singh MJ** (2016) Slot antenna single layer fed by step impedance strip line for Wi-Fi and WiMAX applications. *Electronics Letters* **52**, 1196–1198.
8. **Stutzman WL and Thiele GA** (2012) *Antenna Theory and Design*, 3rd Edn. Hoboken: John Wiley & Sons, Inc.



Amer T. Abed received a degree in Electrical Engineering from College of Engineering, University of Baghdad, 1984. He did his master in Communication Engineering from University of TENAGA, Malaysia and his Ph.D. from UKM, Malaysia. He has wide experience in designing the RF circuit and antennas. Dr. Abed has published 25 papers in ISI journals and two books about antenna design. He has reviewed more than 30 articles in IET and IEEE journals. Currently, he is a lecturer in Communication Engineering Department, Al-M'mamon University College, Baghdad-Iraq.



Mandeep S.J. Singh received his B.Eng. (with honors) and Ph.D. degrees in electrical and electronic engineering from the University of Notrumbria, UK, and Universiti Sains Malaysia, in 1998 and 2006, respectively. From 2006 up to June 2009, he was attached at Universiti Sains Malaysia as a Lecturer. Currently, he is attached to the Universiti Kebangsaan Malaysia as a Professor. Dr. Singh

has published 190 papers in ISI journals. He has reviewed more than 200 articles in impact factors journal.



Aqeel M. Jawad received his B.Sc. in Computer and Communication Eng. from Al-Rafidain University College, Iraq in 2009, his M.Sc. in Electrical Eng. Universiti Tenaga National (UNITEN), Malaysia, 2014. He is currently pursuing the Ph.D. degree with the Department of Electrical, Electronics and Systems Engineering, Faculty of Engineering and Built Environments, Universiti Kebangsaan Malaysia. He is currently with the Department of

Computer and Communication Engineering, as a Lecturer in Al-Rafidain University College, Baghdad-Iraq and head of the communication laboratory.